

Original Article

Image Processing Applied to Doppler Vascular Ultrasonography - Assistance to Carotid Examination Procedures

Wânderson de Oliveira Assis^{1*}, Jonatan Marques dos Santos¹, Pedro Henrique Palauro¹, César Abraham Flores Cisneros Filho¹, Danilo Argollo Pirutti Silva², Bruno Oliveira Cardelino², Alexandre Cesar Fioretti² and Robson Barbosa de Miranda³

¹Electronics Engineering, Instituto Mauá de Tecnologia, Praça Mauá, 01, São Caetano do Sul, SP, Brazil

²Vascular Surgery and Sonography, Faculdade de Medicina do ABC, Santo André, SP, Brazil

³Vascular Surgery and Sonography, Faculdade de Ciências Médicas da Santa Casa de São Paulo, São Paulo, SP, Brazil

***Corresponding author**

Wânderson de Oliveira Assis, Praça Mauá, 01, Bairro Mauá – 09580-900 – São Caetano do Sul – SP, Brazil, Tel: +55-11-97633-2365

Submitted: 03 November 2022

Accepted: 16 December 2022

Published: 18 December 2022

ISSN: 2333-7117

Copyright

© 2022 de Oliveira Assis W, et al.

OPEN ACCESS

Keywords

- Doppler vascular ultrasonography
- Image processing
- Neural networks
- Carotid stenosis

Abstract

This work proposes to integrate engineering and medicine, seeking to assist in color-Doppler vascular ultrasonography, to determine the carotid occlusion percentual (carotid stenosis). The project consists in the development of software which aims to assist the examiner during or after the procedures, employing artificial neural network and image processing resources, such as filtering, contours detection, and character recognizing to extract the relevant data, obtain the diagnosis and be able to automatically generate a medical report with the results. The software acts in diagnosis failures prevention, assisting to make the exam more accurate and less exposed to human mistakes that may invalidate the exam results.

ABBREVIATIONS

[CNES - Cadastro Nacional de Estabelecimentos de Saúde - National Register of Health Establishments; PRF - Pulse Rate Frequency; OpenCV - Open Source Computer Vision Library]; ROI - Region of interest; OCR - Optical Character Recognition; VPS - Velocidade de Pico Sistólica - systolic peak speed; VDF - Velocidade Diastólica Final - diastolic end speed; HSV - Hue, Saturation and Value; ACCD - Artéria Carótida Comum Direita - right common carotid artery, ACID - Artéria Carótida Interna Direita - right internal carotid artery; ACED - Artéria Carótida Externa Direita - right external carotid artery; ACCE - Artéria Carótida Comum Esquerda - left common carotid artery; ACIE - Artéria Carótida Interna Esquerda - left internal carotid artery; ACEE - Artéria Carótida Externa Esquerda - left external carotid artery; AVD - Artéria Vertebral Direita - right vertebral artery; AVE - Artéria Vertebral Esquerda - left vertebral artery; % EAT - Estenose Anatômica Distal - Distal anatomical stenosis; VPS - Velocidade de Pico Sistólica - systolic peak speed; VDF - Velocidade diastólica final - final diastolic speed; CC - artéria Carótida Comum - common carotid artery; CI - Carótida Interna - internal carotid; AE - Artérias esquerdas - left arteries; and AD - Artérias Direitas - right arteries

INTRODUCTION

Advances in technology impact all areas of knowledge,

especially bringing many health benefits. A significant advance in medicine would be impossible, if it were not directly allied with the best that technology can offer.

One of the health fields most dependent on the use of technologies is the diagnostic medicine. In Brazil, the National Register of Health Establishments (CNES) estimates that there are approximately 21 thousand institutions dedicated to diagnostic tests, corresponding to an annual investment of few billions of dollars [1].

In this sense, this work presents the use of technologies to assist medical professionals in order to improve the performance of ultrasound procedures, more precisely focused on the diagnosis based on images in carotid examinations. It is proposed to use image processing algorithms and artificial neural networks in order to facilitate the diagnosis of stenosis as well as assist professionals to perform the exam with greater assertiveness and effectiveness. Several studies show the importance of the results of non-invasive Doppler exams, as a diagnostic tool for moderate or severe carotid stenosis [2]. The publication [3] shows that the diagnosis can be made by monitoring the speed and frequency of the carotid flow. In addition, real-time spectrum analysis of direct carotid Doppler signals substantially improves the diagnostic accuracy of non-invasive identification of operable carotid artery disease [4-6].

As a carotid exam is relatively easy and quick to be done, many clinics in Brazil prioritize quantity over quality, often hiring unprepared professionals in order to minimize their costs, making the data obtained unreal or inconclusive, causing rework to perform a new exam, thus spending more time and resources. In the worst situation, such errors can lead to a wrong diagnosis of the patient's condition, thus subjecting him to unnecessary additional medical diagnostic procedures and even surgeries.

The works [6,7] show the development of image processing algorithms for the detection and automatic generation of curves of the variations in the thickness and diameter of the carotid arteries in sonographic images. The proposal is to compare the results obtained with the application developed with those obtained in commercial ultrasound systems.

In this work, the objectives are similar, however presenting the following differentials in relation to [6,7]:

a) development of a system using Open-Source programming tools that allows the application of the algorithms in real time, in order to assist the examiner during or after the exam, contributing to minimize the incidence of human errors in vascular ultrasound exams with Doppler in the carotid arteries; a system that guarantees the effectiveness and assertiveness of the procedure performed will raise the acceptable quality standards for Doppler exams.

b) development of an algorithm based on image processing and an artificial neural networks application in order to assist the physician in the identification of carotid stenosis with automatic report generation providing a more efficient examination.

MATERIALS AND METHODS

For the development of the work, the concepts of ultrasound applied in vascular Doppler ultrasonography were initially studied. The main difficulties and the most common mistakes in performing the carotid artery doppler exam and in the manipulation of the transducer were investigated.

For the development, Python-based image processing tools were used, which were chosen by taking into account factors such as practicality of use, availability of information and easy access to documentation from software libraries, in addition to the preference for the use of open source tools, making the proposal a low-cost solution.

All research and development steps and the tools used in image processing algorithms are described in the next sections.

IMAGES FOR RETROSPECTIVE STUDY

All images used in the retrospective study for clinical diagnostic purposes were obtained through examinations performed at Clínica Fluxo - Vascular Surgery Clinic. However, the identification of patients was suppressed, so that the data used are anonymous.

ULTRASOUND AN DOPPLER EFFECT

For humans, the audible frequency range is 20 Hz to 20,000 Hz, but each individual has a narrower range that decreases over the course of life. This characteristic of the sound frequency refers to its wave nature in propagation.

The term ultrasound in physics is used to define the frequency range above 20,000 hertz. When a wave interacts with the medium (material) such as a wall or human tissue for example, the following interactions occur: the wave may attenuate during the course and reduce its amplitude; direction change can occur when an oblique beam passing between two materials of different wave velocity (refraction); the wave can disperse in random. However, in the medical ultrasound device, it is the waves refraction that define the distances from human tissues to the device.

Having information on the intensity of the wave returned in comparison with the one sent, in addition to the properties of the propagation medium, it is possible to calculate the distance. In Feldman et al. (2009) [8], (Table 1) is presented, which exemplifies density and speed for different media.

Scattering effect obtained by random reflections in biologic tissues provides the ability to generate texture in the ultrasound image.

Material	Density (kg/m ³)	Speed (m/s)
Air	1,2	330
Greasy	924	1450
Soft Tissue	1050	1540
Bones	1912	4080

Doppler effect received its name from the work of the Austrian physicist Christian Doppler when describing that the relationship between the frequency of light and sound waves is conditioned by the relative movement between source and receiver. In medicine, the devices use the same principle to analyse blood flow. The so-called "doppler frequency" is used to refer to the difference between the frequency sent and received being given by the following relation, according to [9]:

$$fd = (f_r - f_0) = \frac{2 \cdot f_0 \cdot v \cdot \cos \theta}{c} \quad (1)$$

where:

fd: Doppler shift frequency or Doppler frequency; fr: ultrasound frequency; f0: emitted frequency; v: blood flow speed; θ : angle between pulse direction and blood flow (depends on the position of the device); and c: speed in soft tissue (1540 m / s).

Therefore:

$$v = \frac{c \cdot fd}{2 \cdot f_0 \cos \theta} \quad (2)$$

We can separate the ultrasound equipment into two main parts: the transducer and the scanner.

The transducer (or probe) is the part that comes into contact with the patient. Inside it is a synthetic piezoelectric ceramic (usually lead zirconate titanate) which when subjected to a voltage (or pressure) generates a proportional electric field. In pulsed wave Doppler systems. This material works as both a

sender and a receiver. The device applies a voltage oscillating with high frequency on it, generating a sound wave of the same frequency directed at the patient's tissues. There is an interval between these pulses emitted, and in these intervals the waves reflected in the tissue generate a pressure on the ceramic, causing a change in the electric field that is used for the formation of the image.

There are many main types of transducers, but in vascular systems the most used are linear and curvilinear. Linear transducers are mostly used for superficial examinations, such as thyroid and carotid, operating at frequencies between 3 to 16 MHz. Curvilinear transducers are mostly used for deeper organs and vascular vessels, with frequencies usually varying between 3 and 6 MHz.

If the frequency is higher, the resolution of the image will also be higher, but will be smaller the depth of the field of view.

The sonographic scanner is responsible for reading and interpreting the signals received by the probe. With each echo received, it is possible to obtain information; the different strength of echoes provides texture, while time between pulse and echo determines the distance among diverse organs and body structures. By the Doppler effect, is possible to obtain information about flow direction and velocity.

Carotid Artery Doppler and Most Common Mistakes

The carotid arteries that carry blood to head region are divided between common, internal and external carotid arteries. The right carotid arises from the brachiocephalic arterial trunk of the aortic arch.

According to Miranda & Couto (2018) [10], external carotid arteries are responsible for blood supply to the face, scalp, skull and part of the throat located behind the mouth (oropharynx); the internal carotid arteries are larger in diameter than the external carotid and are topographically divided into four segments: cervical, petrous, cavernous and cerebral branches. (Figure 1) shows an illustration of how these vessels are arranged in our body.

The paper "Standardization of equipment and techniques for performing vascular ultrasound exams", written by members of the Department of Cardiovascular Image of the Brazilian Society of Cardiology (Belém et al., 2004) [11] establishes concepts and protocols accepted and used in medicine to perform ultrasound exams Doppler in several parts of the body, including the region of study in this work, the carotid arteries.

First, the examination begins by analysing the artery in a transversal and longitudinal way, as shown in (Figure 2), looking for plaques and irregularities of the vessels and also measuring the maximum intima-media thickness of the common carotid artery (the thicker, the higher cardiovascular risk). Special attention should be paid to the carotid bifurcation between the portion that divides the blood flow to the face and brain, as it is the most common place for plaque formation, due to turbulence in the region. A cross-sectional analysis may quantify the degree of obstruction, the shape of the plaques and whether they are located on the anterior, posterior or lateral wall of the vessel.

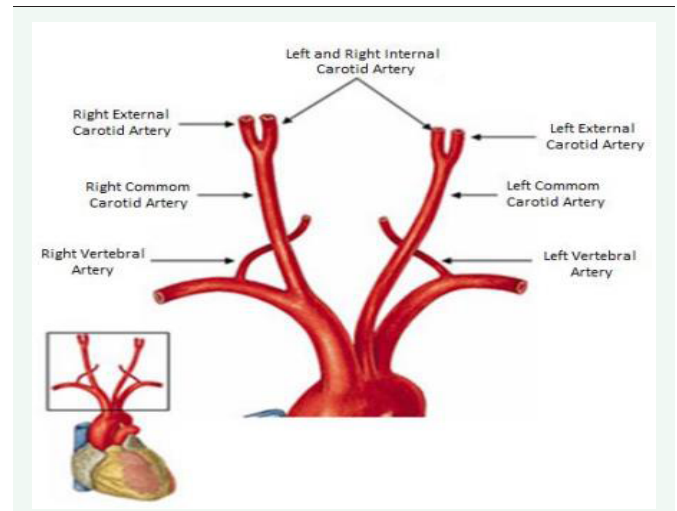


Figure 1 Graphical representation of carotid artery branches (Netter, 2000).

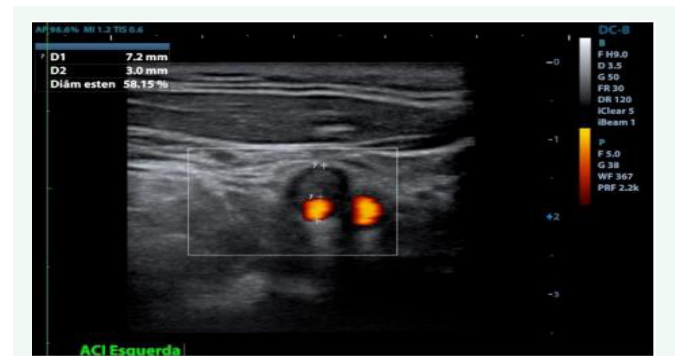


Figure 2 Cross-sectional image of the left internal carotid artery, with measurement of 50-59% stenosis caused by a carotid plaque; "ACI Esquerda" stands for left internal carotid artery.

Following, the analysis is made in a longitudinal way, presented in (Figure 3), where it is possible to check more adequately the extension of the plaques, if any.

The Doppler cursor is not fully aligned to the artery axis but enough aligned to the flow axis. This limit of cursor angulation is due to the equipment characteristics which limit the angulation at that much. Then color Doppler is used, showing the direction of blood flow and areas with greater turbulence through a color scale. With an adequate flow display, the pulsed Doppler is used, which must be positioned as parallel as possible in relation to the flow direction (avoiding going over an angle of sixty degrees in relation to doppler axis) and must not be leaning against the vessel walls, to avoid detecting false turbulences, obtaining the maximum and minimum speeds along the cardiac cycle in the vessel through the spectral graph.

In longitudinal analysis, errors occur when obtaining data, as it is where the operator captures the images and shows the measurements made. The most common errors are:

a) Failure to properly adjust the scale (Pulse Rate Frequency - PRF) when detecting blood flow, leaving the equipment with a

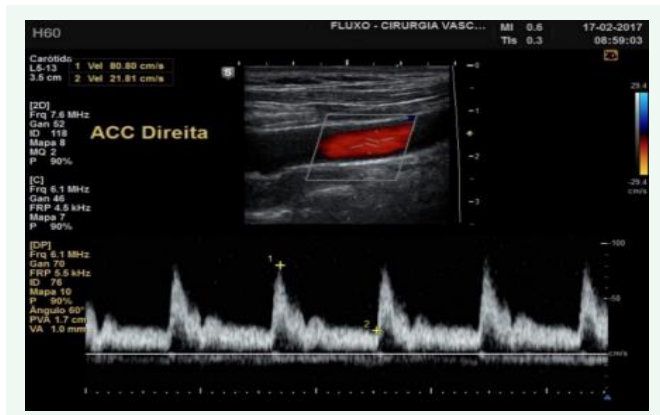


Figure 3 Longitudinal image of the carotid artery, with the flow displayed through the color scale and the spectral speed; “ACC Direita” stands for right common carotid artery.

scanning speed higher or lower than the blood.

- b) Do not use the best possible angle to achieve parallelism during pulsed Doppler, limited to an angle of 60 degrees.
- c) Do not adjust the scale of the spectral speed display, generating an illegible graph.
- d) Failure to correctly position the box, where the Doppler effect occurs in color image, that defines the area to be analyzed, resulting in incorrect flow detection.

Figure 4 shows how harmful scaling errors can be to understanding a doppler exam.

Image Processing Applied to Carotid Artery Ultrasonography with Doppler

For the development, Python-based image processing tools were used, which were chosen taking in account factors such as practicality of use, availability of information and easy access to documentation from software libraries, in addition to the preference for the use of open source tools, making the proposal a low-cost solution.

In addition to the native libraries, the main library adopted in this project, specifically used in image and video processing, is the OpenCV (Open Source Computer Vision Library), widely used for filtering, object recognition, contour detection and, among other applications, including the definition of regions of interest (ROI - Region of interest) where it is associated with the PyTesseract Library through a tool called OCR (Optical Character Recognition), used to extract characters from images..

The integration between the processing software and the operator interface is possible through the PyQt5 library, which allows the internal variables of the software to be associated with the objects contained in the graphical interface and vice versa.

The graphical interface for operating the system was developed using the QtDesigner software, where the saved program is executed at start of application. Despite being a relatively simple and intuitive tool, it is possible to develop advanced interfaces using the available widgets, as well as to create a widget composed of others (when there is a high degree

of repeatability in the use of a set of widgets), for these reasons the QtDesigner proved to be the best solution among the others evaluated.

The interface was developed in such a way that the operator is able to select the mode of operation, adjust the filters as needed, being able to monitor in real time the impact of the parameters on the images under analysis.

All processes related to the treatment of images, such as filtering, displaying objects and extracting data applied to the project, must necessarily depend on at least one region of interest (ROI - Region of interest). When an image is selected for processing, initially its entire length is defined as the region of interest, where other regions can be defined for carrying out different analyses, as shown in (Figure 5).

Considering the objectives of the application, six regions of interest are needed, each with a different functionality. These regions of interest are defined for the Doppler equipment to be used, and the algorithm can be used to determine measurements from exam images collected or at the time of image collection. OCR tools are used to recognize the characters associated with each measurement allowing a comparison with the results determined from the images.

Blood Flow Angle Detection Region

Figure 6 shows the region used to detect the blood flow angle

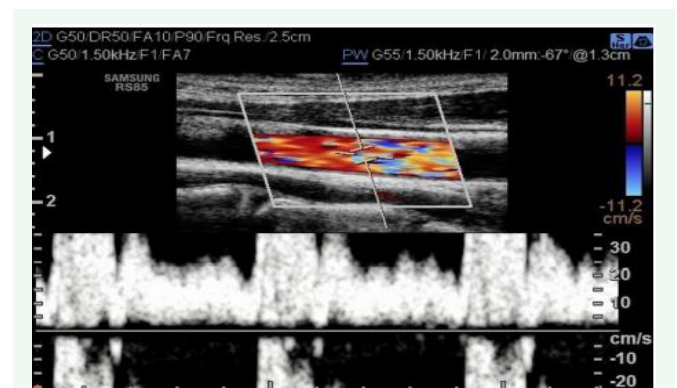


Figure 4 Example of poorly adjusted scales in doppler ultrasonography.

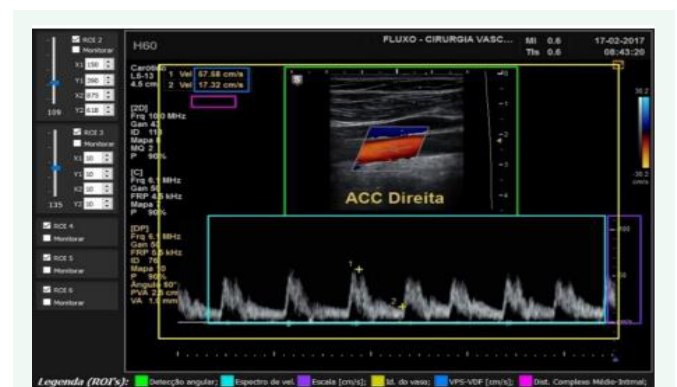


Figure 5 Example of selecting regions of interest at Doppler measurement for the right common carotid artery.

through the vessel, in addition to the automatic estimation and display of the insonation angle. This region must be defined in such a way as to involve the image obtained by the device, where the operator uses the color resource on which filters have been applied that allow estimating the correct angle for the acquisition of the systolic peak speed (VPS) and diastolic end speed (VDF).

Speed Spectrum Region

After the cursor is correctly fixed, it is possible to obtain the blood flow velocity curve (Figure 7). Thus, this region is used to extract the speeds of interest after obtaining local maximum and minimum points on a curve defined by cycles, either manually or automatically, acting directly in conjunction with the scale detection region.

For the detection of speeds to be done correctly, it is necessary to correlate the coordinates of the points obtained in the speed spectrum region with the speed scale. For this, the same vertical dimension is adopted for the two regions, making it possible for both regions to collect data in the same order of magnitudes. The scale region is responsible for identifying the values contained therein, and then determining its vertical coordinates. Thus, it is possible to determine the speeds through the correlation between the y coordinates of the values identified in the scale (data in pixels), the values obtained in it (data in cm / s) and the coordinates of the points selected in the speed spectrum.

Thus, a mathematical expression capable of converting a given point y (pixel) to its equivalent value in speed (cm / s) was deduced:

$$V(P) = (\Delta_y - P) \cdot f_e \quad (3)$$

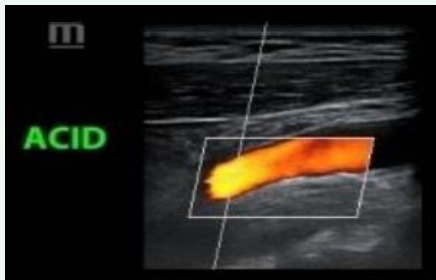


Figure 6 Region of Interest for Detecting the Insonation Angle; "ACID" is the right internal carotid artery.

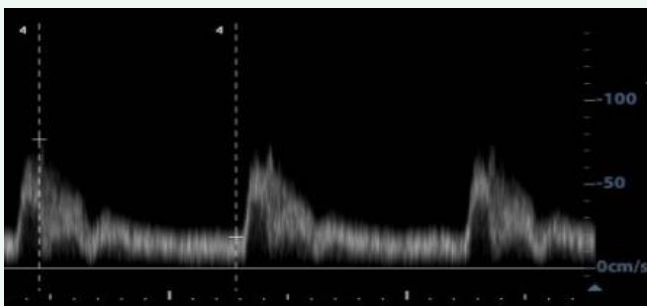


Figure 7 Speed spectrum for data and scale extraction.

where:

P : Pixel vertical coordinate of the point to be converted (Pixel);

Δy : Vertical dimension of the region of interest (Pixel);

f_e : Full scale, in which its value indicates how much each unit in Pixel represents after conversion to the speed scale (cm/s.Pixel)).

The full scale can be calculated using the following expression:

$$f_e = \frac{|v_A - v_B|}{|y_A - y_B|} \quad (4)$$

where:

v_A : Highest speed contained in the scale (cm/s);

v_B : Lowest speed contained in the scale (cm/s);

y_A : Pixel coordinate associated with the speed value v_A (Pixel);

y_B : Pixel coordinate associated with the speed value v_B (Pixel).

Blood Vessel Identification Region: Among all the defined regions, the blood vessel identification region has the largest area. Considering that the equipment operators must label the images with the name or abbreviation of the vessel to which they refer, it is common to have disagreements as to the most appropriate location for the insertion of the text. Thus, this region must be able to locate the text anywhere on the image, even the most inconvenient ones. Its dimensions are usually slightly smaller than the dimensions of the image, where the filtering should be less sensitive to the presence of other texts that do not present relevant information.

Speed Collection Region

Region defined only for the collection of the intimal-media distance (not considered in all exams).

Image Filtering

The implemented filters allow you to convert the color system of the original image using OpenCV. Among the systems, there are the gray scale, the HSV system formed by the hue, saturation and value components respectively, in addition to the binary system in which a threshold is defined, where values above or below this threshold are considered black or white. These filters, exemplified in (Figure 8), are extremely important for detecting certain colors of interest contained in the images, in addition to extracting contour points from the images obtained by the transition between one color and another. This transition is observed when the parameters of any of these filters are changed.

Using the convenient filters (Gonzales & Woods, 2010) [12], it is possible to display the contours in the image, so that the operator is able to find the best adjustment of the HSV parameters in such a way that the points are in fact surrounding the object of interest in the image, where it process can be called filters calibration.

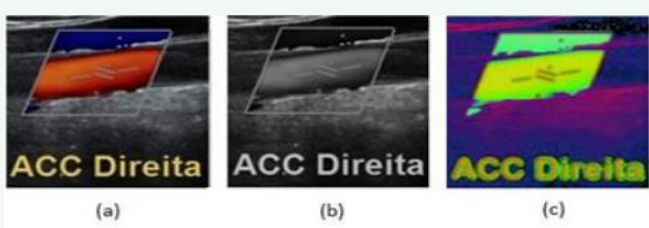


Figure 8 Application of color filters. (a) Original image; (b) Gray image; (c) HSV image; "ACCD" stands for right common carotid artery.

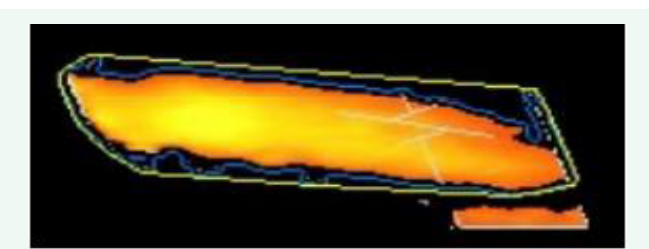


Figure 9 Example of calibrating contour display and convex outline in OpenCV filters.

Figure 9 illustrates an example of filtering using the algorithms available in OpenCV to obtain the image outline (in blue) and determine dimensions from the convex outline (in yellow).

Using the filtering and contour detection features, it is possible to detach the walls of the carotid artery within the colored box, and to adjust as centrally as possible a rectangle or an ellipse that surrounds the entire highlighted region (Figure 10), where lines of the horizontal axes of these adjusted geometries bring with them the approximate direction of blood flow that travels the vessel in a very satisfactory way, coinciding with the point and angle at which the examiner must position the cursor to extract the speed spectrum (Figure 11), therefore serving as a guide and reducing the likelihood of errors.

A third type of contour was developed specifically for

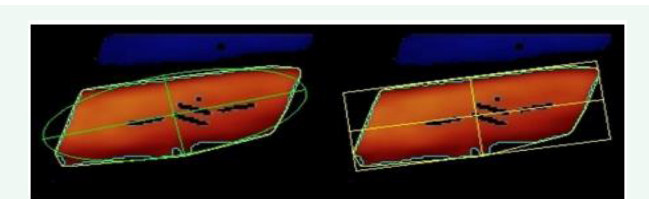


Figure 10 Comparison between elliptical and rectangular adjustments.

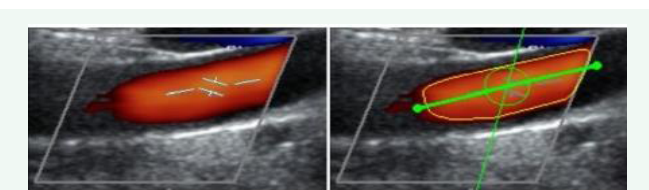


Figure 11 Comparison between the positioning of the cursor during the exam (on the left) and the automatic adjustment (on the right).

graphical analysis of the speed spectra. Since the background of the original figure (Figure 12) is dominated by black pixels, and the speed spectrum displayed in shades of gray, a logic has been developed that verifies strategic points contained in the asymptotic lines that intersect all the contour points, in order to ensure that the plot of the new points corresponded to the upper contour.

DIAGNOSIS BY IMAGE PROCESSING

For determine the percentage of the patient's stenosis, it is necessary to gather all the data obtained in a set of ten images, where these data are subjected to a series of mathematical calculations and the results are evaluated according to a table of values and criteria. Therefore, the system must be able to extract the numerical values from these images, as well as correctly associate them with the vessel from which the speeds were obtained.

Applying the character identification algorithm to well-defined and properly filtered regions of interest, the velocity values are collected at the same time as the blood vessel identification. At the end of this cycle, the data is associated so that the process is repeated for the other images.

After scanning all the images that make up the exam, a report is generated using an algorithm that performs all the calculations and crosses of data to determine the patient's stenosis percentage (Figure 13), avoiding possible human errors in the process of data entry and report preparation, where: ACCD - right common carotid artery, ACID - right internal carotid artery; ACED - right external carotid artery; ACCE - left common carotid artery, ACIE

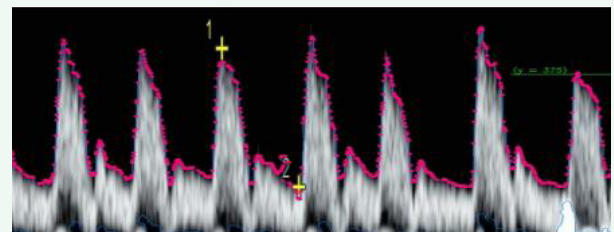


Figure 12 Contour points on the speed curve.

Paciente nº 2			Relatório	
ART	VPS [cm/s]	VDF [cm/s]	AE	AD
ACCD	80.8	21.81	VPS (CI/CC)	
ACID	69.91	26.81	0.55	0.87
ACED	156.7	32.21	VPS CI/VDF CC	
ACCE	106.62	27.53	2.13	3.21
ACIE	58.58	21.09	VDF (CI/CC)	
ACEE	244.84	43.53	0.77	1.23
AVD	43.13	9.91	% EAD	
AVE	51.37	18.93	< 50 %	< 50 %

Figure 13 Example of results obtained after collecting data and performing calculations.

Table 2: Classification of groups associated to stenosis percentages.

Group	% Stenosis
1	< 50%
2	50 – 59%
3	60 – 69%
4	70 – 79%
5	80 – 89%
6	> 90%

Table 3: Criteria for classification of percentage of stenosis.

%EAT	VPS (cm/s)	VDF (cm/s)	VPS CI/ VPS CC	VPS CI/ VDF CC	VDF CI/ VDF CC
< 50%	< 140	< 40	< 2,0	< 8	< 2,6
50 - 59%	140 - 230	40 - 69	2,0 - 3,1	8 - 10	2,6 - 5,5
60 - 69%		70 - 100	3,2 - 4,0	11 - 13	
70 - 79%	>230	> 100	> 4,0	14 - 21	
80 - 89%		> 140		22 - 29	> 5,5
> 90%	> 400		> 5,0	> 30	

Abbreviations: % EAT - Estenose Anatômica Distal - Distal anatomical stenosis; VPS - Velocidade de Pico Sistólica - systolic peak speed; VDF - Velocidade diastólica final - final diastolic speed; CC - artéria Carótida Comum - common carotid artery; CI - Carótida Interna - internal carotid

- left internal carotid artery; ACEE - left external carotid artery; AVD - right vertebral artery and AVE - left vertebral artery.

Table 2 defines the groups associated with the percentage of stenosis used to define the diagnosis.

Table 3 defines the criteria for classification associated with the percentage of stenosis based on the results of the exam (Freire et al., 2015) [13] where: % EAT: Distal anatomical stenosis; VPS: systolic peak speed; VDF: Final diastolic speed; CC: Common carotid artery; CI: Internal carotid.

The columns in the table correspond to the different evaluation criteria and their respective relevance for the final diagnosis, using the collected systolic and diastolic velocities, and some relationships between them. The lines correspond to the percentage of occlusion of the carotid arteries, that is, the set of values obtained from the velocities will result in a certain degree of stenosis.

AUTOMATIC DIAGNOSIS BY ARTIFICIAL NEURAL NETWORKS

A possible approach for obtaining the diagnosis could be the direct analysis of the data obtained in the exam and using Table 3. The main benefits of employing an artificial neural network algorithm to identify the degree of stenosis in patients are:

a) identification when the patient has worrying levels, allowing special attention from the professional who is performing the exam, including when due to inaccuracies or errors in the measurements, the data tend to present inconclusive results;

b) real-time identification when a measurement is a threshold between two percentage ranges of EAT presented in Table 3;

again, the performance of the professional will allow to obtain more precise values; additionally, the results in this case will allow indicating the degree of relevance within the diagnostic ranges (for example, diagnosis between groups 2 and 3).

For the creation of the artificial neural network algorithm in order to obtaining a diagnosis, different networks were evaluated, which were trained using a set of data obtained in examinations of several patients, which were not identified to preserve privacy. The data used were peak systolic and final diastolic speeds for the internal and common, right and left carotid arteries, with independent diagnoses for the right and left carotid arteries, being considered as outputs with value 1 for patients who presented stenosis less than 50%, value 2 for patients with stenosis between 50 and 59%, value 3 if between 60 and 69%, value 4 if between 70 and 79%, value 5 if between 80 and 89% and finally value 6 if stenosis is above 90%.

Unfortunately, the number of samples used in training was relatively low due to the number of exams available.

Using the Neural Networks toolbox of the Matlab software, a Feed-forward Backpropagation network was created, consisting of two layers, the first consisting of ten neurons and using the LogSig (Log-sigmoid transfer function) activation function, while the second layer uses only a neuron and TanSig activation function (Hyperbolic tangent sigmoid transfer function). The implemented configuration is shown in (Figure 14). This was the configuration that presented the best results.

In the network, the input variables E1, E2, E3 and E4 represent, respectively, peak systolic speed of the internal carotid, final diastolic speed of the internal carotid, systolic peak speed of the common carotid and final diastolic speed of the common carotid.

After training the network, the parameters responsible for producing an output state (classification) associated with the set of input data are generated, namely:

(n, i) : Input Weights, where n is the neuron index and i is the input index;

(1): Input Weights for output neuron (multiply the output of the 1st layer neurons), where j is the index of the supplying neuron;

(n) : Bias, where N is the layer number.

RESULTS AND DISCUSSION

The system was used as a tool to facilitate the examination and the data obtained were validated, obtaining the results summarized below:

a) Angle of insonation - the accuracy of the automatic determination of angles of blood flow and insonation is strongly dependent on the parameters adjusted by the HSV filter, since it is possible to distinguish the colors of interest (predominantly blue and red tones) and to remove the rest. Given the variation in color tone for each image, a standardized value was reached for the HSV parameters in order to contemplate the largest possible number of images, but it is worth noting that several improvements can be made for each specific equipment, making the parameterization self-adjusting, resulting in a more viable operational interface for

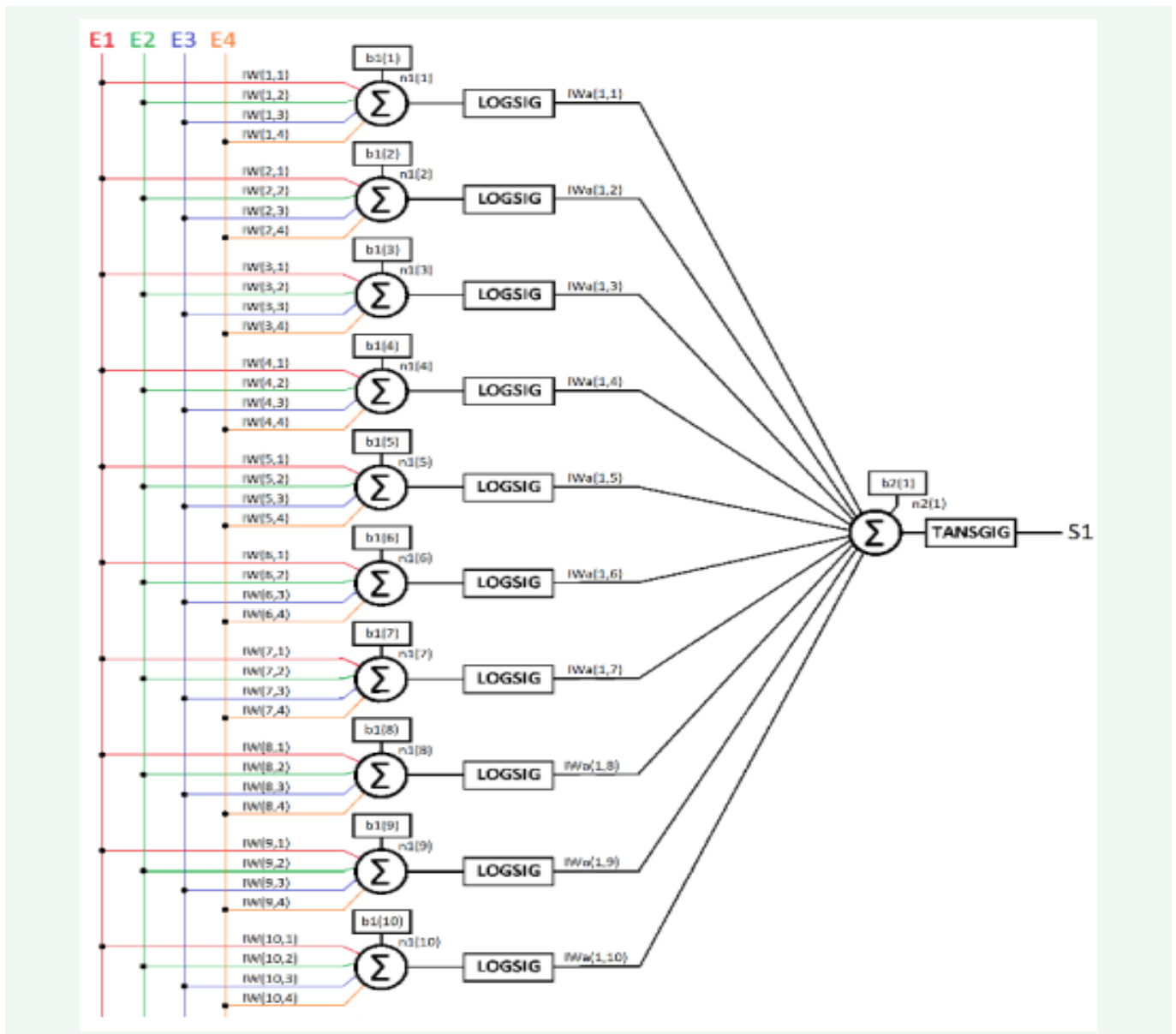


Figure 14 Construction of the neural network, with output classified from the data of four continuous input variables.

future system operators. (Figure 15) demonstrates the proximity of the resulting automatic angulation, when the parameters are properly adjusted.

b) Speed scale - The validation process of automatic scales consists, first, of manually positioning the speed lines on the y coordinate corresponding to the number extracted from the scale shown in the original figure (Figure 16), and comparing the error between these values and those obtained through the lines. The algorithm analyzes a complete cycle and obtains the maximum peak within the cycle. Measurements are performed automatically by the image processing algorithm and can be validated because they are very close to the values obtained manually from the instruments. The errors present in the tables can be justified by the y dimension of the regions of interest referring to the scale and speed curves, where larger dimensions result in a lower scale value, contributing significantly to the

increase of the scale accuracy. To illustrate, considering 08 exam images, the percentage errors presented for the measurements in the upper value of the scale had a maximum error of 0.58% and an average error value of 0.0073%. In the lower intermediate scale (half of the curve) there was a maximum error of 2.32% and an average error of 0.55%. Therefore, the percentage error between the value measured in the algorithm with automatic scale and the one obtained manually, by placing the cursor on the graph, proved to be quite small. Thus, the results obtained were considered reasonably accurate.

The maximum absolute error between the actual peak systolic and straight line speeds automatically adjusted in the algorithm was 7.50 and the average 3.109; the maximum absolute error between the actual final diastolic speeds and the adjusted straight lines in the algorithm was 5.92 and the average 3.448.

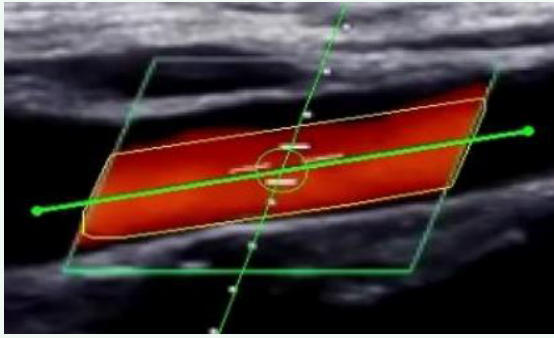


Figure 15 Angle of insonation - Example of results obtained after collecting data and performing calculations.

The maximum absolute error between the actual peak systolic and straight line speeds automatically adjusted in the algorithm was 7.50 and the average 3.109; - the maximum absolute error between the actual final diastolic speeds and the adjusted straight lines in the algorithm was 5.92 and the average 3.448.

c) Automated diagnosis - The final diagnosis is obtained by means of a classifying algorithm, in which all the analysis criteria are inserted. The data extracted from the images are organized, and then they are submitted to the evaluation of the system, according to Table 3. In order to obtain the diagnosis, it is necessary that the system operator select the set of images obtained in the exam and fill in the fields contained in the "Examination data" area, where the option to enable the report must be checked, the file destination must be defined then click on the "Generate diagnosis" button. Therefore, the developed tool allows the operator easily produce the report related to the exam, but with the automatic diagnosis being defined by the algorithm. At the end of the process, the diagnostic table similar to that shown in (Figure13), being filled in automatically, with the abbreviated identifications of the arteries and their associated associated speeds. For the criteria in which it is necessary to calculate the relationship between speeds, partial results can be consulted in columns AE (Left arteries) and AD (Right arteries). The final result can be consulted directly on the application interface, and corresponds to the values of anatomical distal stenosis for the right and left arteries. The final report (Figure 18) is saved in the selected directory, in which will be a folder with the patient's name containing a text file also identified with the patient's name, in order to provide greater organization on the part of the user, in view of the large number of files you will be working with.

d) Automated diagnosis by artificial neural network - In order to validate the use of the artificial neural network algorithm, simulations were carried out with 34 exams (small number and in which it was necessary to include the training data, which is not a convenient practice). Table 4 shows the results associated with the percentage groups of stenosis comparing cases of real diagnoses and those obtained in the validation of the algorithm. It is observed that the classification obtained by the artificial neural network practically coincides with the results of the groups defined by the real diagnosis, assigned by professionals in the medical field, presenting correctness in all diagnostic results if we consider that the values obtained at the output of the neural

network have an error margin of ± 0.1 in the ranges allowed for each solution (values 1 to 6 expected at the output for each diagnostic range of stenosis).

CONCLUSION

Based on the results obtained, it is possible to affirm that the resources of analysis and image processing, despite being already largely incorporated into medicine, still represent a great potential for development. One of the main pillars of the significant progress achieved in the different areas of medicine is the development of dedicated equipment and instrumentation, increasingly modern technologies created from specific demands.

Table 4: Results of automatic classification using artificial neural network.

Examination	Group	Classification	Stenosis
1	1	10,006	< 50%
2	1	10,014	< 50%
3	1	10,003	< 50%
4	1	10,016	< 50%
5	1	10,012	< 50%
6	1	10,049	< 50%
7	1	10,230	< 50%
8	1	10,043	< 50%
9	1	10,043	< 50%
10	1	10,704	< 50%
11	1	10,015	< 50%
12	1	10,176	< 50%
13	1	10,354	< 50%
14	1	10,009	< 50%
15	1	10,007	< 50%
16	3	29,953	60 - 69%
17	1	10,106	< 50%
18	2	10,043	50 - 59%
19	1	10,426	< 50%
20	1	10,119	< 50%
21	1	10,353	< 50%
22	1	10,100	< 50%
23	1	10,169	< 50%
24	1	10,195	< 50%
25	1	10,009	< 50%
26	1	10,032	< 50%
27	1	10,344	< 50%
28	1	10,101	< 50%
29	4	39,459	70 - 79%
30	1	10,108	< 50%
31	4	39,620	70 - 79%
32	1	10,023	<50%
33	1	10,006	<50%
34	1	10341	<50%

The developed application makes it possible to compare its independent results with the results collected by the operator of the ultrasound device, in order to avoid that there are significant discrepancies, to the point that later sets of illegible images are delivered for medical analysis, making it necessary to carry out further tests. The obtaining of the insonation angle limit is another critical point of analysis, serving as an excellent reference when used in real time mode, or simply as a post-examination tool, being able to indicate whether the collected data are valid and were collected correctly. This item can be used as a reference to indicate to the operator if the exam is being performed correctly or if a review is needed in the procedure.

And finally, the automated diagnostic tool, which processes the data in an impersonal manner and prevents errors of human nature from being made during the process, performing all the calculations and generating each report within approximately ten seconds, in a practical and organized manner.

The preliminary results obtained by the artificial neural network demonstrate that the method has potential for application in the classification of the percentage of stenosis, enabling convergence for a correct diagnosis, but the extreme accuracy expected to make its implementation feasible depends primarily on a large availability of data, so that they are separated into two sets, for training and validation.

ACKNOWLEDGEMENTS

Sincere thanks to the team of professors from the Instituto Mauá de Tecnologia and doctors from Faculdade de Medicina do ABC and from Faculdade de Ciências Médicas da Santa Casa de São Paulo, who collaborated a lot in guiding and collecting data from the exams.

REFERENCES

- Campana, G A, Oplustil, C P, Faro, L B, Tendências em Medicina Laboratorial. *Jornal Brasileiro de Patologia e Medicina Laboratorial*, v. 47, no 4, Rio de Janeiro, Agosto, 2011.
- Santos SN, Monica Luiza de Alcantara, Claudia Freire, Armando Cantisano. Posicionamento de Ultrasonografia Vascular do Departamento de Imagem Cardiovascular da Sociedade Brasileira de Cardiologia – 2019. *Arquivos Brasileiros de Cardiologia*. 2019; 112.
- Hatle L, Angelsen B A, Tromsdal A. Non-invasive assessment of aortic stenosis by Doppler ultrasound. *Br Heart J*. 1980; 43: 284-292.
- Lee, W. *General Principles of Carotid Doppler Ultrasonography*. *Ultrasonography*. 2014; 33: 11-17.
- Edward G Grant, Carol B Benson, Gregory L Moneta, Andrei V Alexandrov, J Dennis Baker, Edward I Bluth, et al. Carotid artery stenosis: gray-scale and Doppler US diagnosis--Society of Radiologists in Ultrasound Consensus Conference. *Radiology*. 2003; 229: 340-6.
- Higa M, Pilon P E, Lage S G, Gutierrez MA. A Computational Tool for Quantitative Assessment of Peripheral Arteries in Ultrasound Images. *36th Annual Computers in Cardiology Conference (CinC)*. Park City, UT, USA, 2009; 13-16.
- Higa M. A Métodos para Quantificação da Artéria Carótida em Imagens de Ultrassom Modo-B e Doppler. *Electrical Engineering Masters Dissertation*. Escola Politécnica da Universidade de São Paulo, São Paulo, SP, Brasil, 2009.
- Myra K Feldman, Sanjeev Katyal, Margaret S Blackwood. *US Artifacts*. *Radiographics*. 2009; 29: 1179-89.
- Andrew A Pellett, Edmund K Kerut. *The Doppler Equation*. *Echocardiography*. 2004; Feb;21: 197-8
- Miranda RB, Couto VAP. *Doppler das Artérias: Carótidas e Vertebrais*. São Paulo, SP, Brasil: Di Livros, 2018.
- Belém LHJ, Jorge Ilha Guimarães. *Normatização dos Equipamentos e das Técnicas para a Realização de Exames de Ultrasonografia Vascular*. Sociedade Brasileira de Cardiologia. *Arq. Bras. Cardiol*. 2004; 82.
- Gonzales RC, Woods RE. *Processamento Digital de Imagens*. São Paulo: Pearson Prentice Hall, 2010.
- Cláudia Maria Vilas Freire, Monica Luiza de Alcantara, Simone Nascimento dos Santos, Salomon Israel do Amaral, Orlando Veloso, Carmen Lucia Lascasas Porto et. al. Recomendação para quantificação pelo ultrassom da doença aterosclerótica das artérias carótidas e vertebrais. Grupo de trabalho do Departamento de Imagem Cardiovascular da Sociedade Brasileira de Cardiologia – DIC – SBC. *Arq Bras Cardiol: Imagem cardiovasc*. 2015; 28: e1-e64.